Proceedings of RAAD'03, 12th International Workshop on Robotics in Alpe-Adria-Danube Region
Cassino May 7-10, 2003

ON MODEL-BASED CONTROL OF HYDRAULIC ACTUATORS

Panagiotis Chatzakos and Evangelos Papadopoulos

Department of Mechanical Engineering
National Technical University of Athens
Heroon Polytechniou 9, 15780 Athens, Greece
email: pchatzak@central.ntua.gr, egpapado@central.ntua.gr

ABSTRACT- Electrohydraulic servosystems exhibit highly nonlinear behavior to the effect that classical linear controllers, e.g., PD, usually achieve a limited performance. Load static and dynamic parameters variations are also contributing to the limitation of their position and force tracking performance. This paper presents a model-based controller applied to a fully detailed model of an electrohydraulic servosystem aiming at improving its position and force tracking performance. Fluid, servovalve, cylinder and load dynamics are taken into account. Simulation results show the strategy to be promising in controlling hydraulic servoactuators. The approach can be further extended to the control of hydraulically driven manipulators and simulators.

Keywords: Hydraulics, Electrohydraulic Servosystem, Servovalve, Hydraulic Dynamics, Model-Based Control.

INTRODUCTION

Many mobile, airborne and stationary applications employ hydraulic control components and servosystems. Hydraulic servosystems can generate very high forces, exhibit rapid responses, and have a high power-to-weight ratio compared to other technologies. On the other hand, they exhibit a significant nonlinear behavior due to the nonlinear flow/pressure characteristics, oil compressibility, time varying eigenfrequency behavior, nonlinear transmission effects, flow forces acting on spool and friction, which is not only largely uncertain but is greatly influenced by external load disturbances.

In recent years, many control schemes that do not depend on operating point linearizations have been proposed to improve hydraulic servosystem performance [1]. This approach sacrifices controller performance in favor of its robustness, while another study uses a classical analysis to point out that common PID controllers are inadequate for force tracking due to hydraulic system fundamental limitations, [2]. Pressure feedback has been used to improve the performance of classical PD controllers, [3]. Various other controllers from neural to adaptive have maintained good performance of electrohydraulic servosystems, [4-6]. However, the response of such a system heavily depends on the load and its variations, thus the performance and robustness of neural controllers is an issue. The nonlinear adaptive force control scheme of an active suspension achieves better performance than conventional linear controllers, [5], where only cylinder uncertainties were considered. The same applies to [7] where the back-stepping approach of [5] was extended from force to motion control using a hydraulic actuator with a three-way valve. Load uncertainty parameters were taken into account to result in a precise motion of a single-rod hydraulic actuator, [6].

A hybrid position/ force control scheme was proposed, using a time-delayed dynamic inversion and a Lyapunov analysis, respectively, [8. 9]. In these papers, either the servovalve leakages have been neglected or unreasonable acceleration estimations have been used in the feedback control law by twice differentiating the actual ([8]) or desired ([9]) piston position. Also, the cylinder output force is calculated from the pressure drop across the cylinder and therefore, not at the load.

Another time-delayed scheme is introduced for torque tracking in constrained and free motion for a hydraulic robot with proportional valves, [10]. The dynamics of the hydraulic servosystem were replaced by a simple time-delay, while a force sensor measured the actual torque. In constrained motion, where the dynamics of the system are simplified due to the small piston rod movement, force tracking is quite good. However, the reduction of system dynamics to a simple time-delay results in poor force tracking in free motion. A model-based controller of a hydraulically driven manipulator was studied but the feedforward controller terms are calculated using desired and not actual positions, leading to poor results, [11].

In this paper, a fully detailed model of an electrohydraulic servosystem, which includes fluid, servovalve, servoactuator and load dynamics, is presented and used for evaluating the proposed model-based controller for force tracking control, both in free and constrained motion. It also compares its position tracking performance to that of a classical linear controller, using intensive simulations. Load dynamic and static parameters are varied widely so as to test the proposed controller in various load conditions. Simulation results show the technique to be promising in providing robust position and force control and in extending the approach to hydraulically driven

manipulators and motion platforms. The paper is organized as follows. Following system physical modeling, a model-based controller for both constrained and free motion is developed, and simulation results are provided. Comparisons against classical control are presented.

PHYSICAL MODELING

The development of an accurate dynamic model for a hydraulic servosystem is important for understanding the system and for developing a robust controller. To this end, a description of the dynamics for the fluid subsystem, the servovalve, the cylinder and the load is required.

Fig. 1 shows a hydraulic servoactuator, including a servovalve, a cylinder, a force sensor and an inertial load. The dynamic model must also take into account the power supply (a variable displacement constant pressure pump) and transmission line dynamics. Small loses due to filters or other hydraulic components are lumped into line losses.

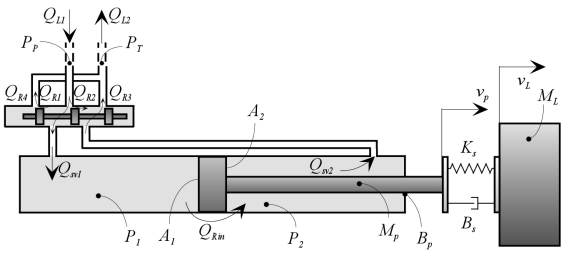

Fig. 1. Schematic model of hydraulic servoactuator.

The model of the hydraulic subsystem was developed using Linear Graphs ([12]), which allow a systematic generation of system state-space equations, using three sets of equations, namely the elemental equations and the compatibility and continuity equations. In hydraulic systems, element equations describe the relationship between pressure and flow for the elementary hydraulic elements such as the inertial, capacitor and resistive element. Compatibility equations result in pressure drop equations along a closed circuit, while continuity equations result in flow continuity at systems nodes or closed surfaces.

The model, in its detailed form is useful in understanding the physical phenomena in the system and can be used to evaluate controller performance in simulation. Modeling of several key components is discussed next.

Hydraulic Unit and Transmission Lines

The custom-made constant pressure power unit, equipped with a PARKER PVP41 Series variable displacement piston pump, is modeled as a source of constant pressure, while transmission lines are modeled as an inertance, a resistance and a capacitance connected in a T-configuration (lump-parameter line model). This is a suitable description for simulation purposes provided that the frequency of oscillations in the system is significantly less than that corresponding to wave propagation, [13].

Servovalve

The MOOG G761 Series servovalve is a high performance two-stage design valve. The output stage is a closed center, four-way, sliding spool, while the pilot stage is a symmetrical double nozzle and flapper, driven by a torque motor. Since its natural frequency is orders of magnitude higher than the desired closed loop bandwidth, only its orifices resistive effects was taken into account, and is described by ([14])

$$P_R = C_R \cdot Q_R \cdot |Q_R| \qquad (1)$$

where P_R is the pressure drop across the orifice, Q_R is the flow through the orifice and the coefficient of C_R is a function of fluid density ρ, the orifice area A and the discharge coefficient C_d,

$$C_R = \rho / \left(2 \cdot {C_d}^2 \cdot A^2\right) \qquad (2)$$

The valve spool position modulates the orifice area, which in turn affects the magnitude of C_R, and is controlled by an input voltage command. The square root of the inverse of the orifice resistance, called hereafter servovalve orifice hydraulic conductance G_R is defined as $G_R = C_R^{-1/2}$.

The four symmetric and matched servovalve orifices make up a four-legged flow path of four nonlinear resistors modulated by the input voltage and thereby the servovalve is modeled as the hydraulic equivalent of a Wheatstone bridge. Two schematic model versions of the servovalve are given in Fig. 2 where the orifice leakage is taken into account (Fig. 2.b) and neglected (Fig. 2.a).

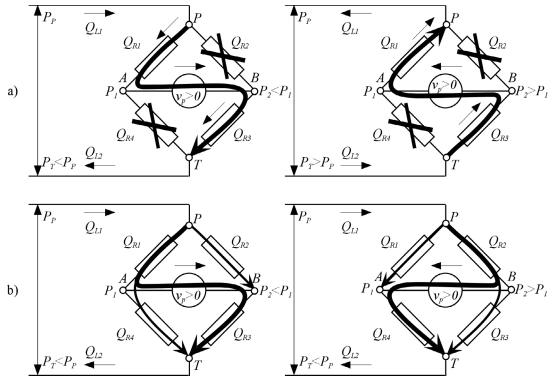

Fig. 2. Schematic model of servovalve, when orifice leakage is (a) neglected and (b) taken into account.

In the latter case, only two nonlinear resistors are required to build the servovalve model. However, in this case and for simulation purposes, two dynamic models should be used for the servovalve, in order to allow for both forward and backward motions of piston rod. In other words, to have the sign of rod velocity changed, the servovalve must be able to reverse the oil flow direction, as required by the headside and rearside piston gyrators equations, respectively, see Fig. 3.

$$\begin{bmatrix} F_{A_1} \\ v_p \end{bmatrix} = \begin{bmatrix} A_1 & 0 \\ 0 & 1/A_1 \end{bmatrix} \begin{bmatrix} P_1 \\ Q_{A1} \end{bmatrix} \quad (3)$$

$$\begin{bmatrix} F_{A_2} \\ v_p \end{bmatrix} = \begin{bmatrix} -A_2 & 0 \\ 0 & -1/A_2 \end{bmatrix} \begin{bmatrix} P_2 \\ Q_{A2} \end{bmatrix} \quad (4)$$

where A_1 and A_2 are the piston areas at headside and rearside, respectively (see Fig. 1).

This reversal of flow can be obtained either by using two pressure sources, one set always at pump pressure, while the other set always at tank pressure, or by assuming that the "polarity" of the pressure source changes according to the sign of the input voltage sent to the servovalve.

Contrarily, modeling the servovalve as a hydraulic bridge the topology of the real servovalve is respected and the servovalve model is the same for any input command. The direction of oil flow, i.e., the direction of rod motion, is obtained by following the appropriate flow path, which is controlled by the input command sign. However, this modeling choice introduces numerical stiffness problems, because two of the four resistances of the bridge are always very large, [15]. On the other hand, it also introduces the hydraulic damping of the real system, caused by the residual flows leaking through the orifices when the servovalve is closed. This modeling technique for the servovalve is followed in this paper.

Due to symmetry and match of the orifices the magnitude of C_R of any orifice can be obtained from one orifice for any input command. The other orifice resistances are calculated as

$$\begin{aligned} C_{R1}(i_{sv}) &= C_{R3}(i_{sv}) = C_{R3}(-i_{sv}) = C_{R,P\to A} \\ C_{R2}(i_{sv}) &= C_{R4}(i_{sv}) = C_{R1}(-i_{sv}) = C_{R,P\to B} \end{aligned} \quad (5)$$

where $C_{R,P\to A}$ and $C_{R,P\to B}$ are the orifice resistances of each flow path, see Fig. 2. As shown in previous works, experimental data for the servovalve orifice conductances can be obtained and a polynomial representation of G_R can be found using curve fitting algorithms, [16], [17].

Servocylinder

The servovalve drives a custom-made double-acting single-ended MOOG servocylinder with an internal analog R-Series MTS linear displacement transducer and special low friction seals and glands. Because of the latter, the stick-slip effect is minimal and the piston friction is only due to Coulomb and viscous friction. The piston areas are not equal, thus two gyrators are used to describe the conversion of pressure to force, see Fig. 3. The piston gyrator equations are given by Eqs. (3) and (4).

System Full Model

The graph of the full model of the hydraulic servosystem is shown in Fig. 3. This also includes an inertial load and a force sensor between the load and the rod, which is modeled as a first order system with high stiffness and damping. The application of continuity and compatibility laws, along with individual elements equations, leads to a set of nine nonlinear first order differential equations as follows,

$$\dot{P}_{L1} = \left((P_s - P_{CL1})/R_{L1} - Q_{L1}\right)/C_{L1} \quad (6)$$

$$\dot{Q}_{L1} = \left(P_{CL1} - P_{R1} - P_1\right)/I_{L1} \quad (7)$$

$$\dot{P}_1 = \left(Q_{L1} - A_1 v_p - Q_{R2} - Q_{R4} - R_{in} P_L\right)/C_1 \quad (8)$$

$$\dot{P}_2 = \left(Q_{R2} + Q_{R4} + A_2 \cdot v_p - Q_{L2} + R_{in} P_L\right)/C_2 \quad (9)$$

$$\dot{Q}_{L2} = \left(P_2 - P_{R3} - P_{CL2}\right)/I_{L2} \quad (10)$$

$$\dot{P}_{CL2} = \left(Q_{L1} - P_{CL2}/R_{L2}\right)/C_{L2} \quad (11)$$

$$\dot{v}_p = \left(A_1 P_1 - A_2 P_2 - B_p v_p - B_s\left(v_p - v_L\right) + -F_{Ks} - F(v_p) - F_{gp}\right)/M_p \quad (12)$$

$$\dot{F}_{Ks} = K_s\left(v_p - v_L\right) \quad (13)$$

$$\dot{v}_L = \left(F_{Ks} + B_s\left(v_p - v_L\right) - F_{gL}\right)/M_L \quad (14)$$

where $P_L = P_1 - P_2$ is the load pressure drop and the remaining variables are defined in Table I.

Table I. Nomenclature.

Variable	*Definition*
R_L, C_L, I_L	Resistance, capacitance and inertance of lines
Q_L, Q_{sv}, Q_A	Flow in lines, to/from cylinder, due to motion
P_s, P_P, P_T	Supply and servovalve inlet/outlet pressures
C_1, C_2	Fluid capacitance in cylinder chambers
P_1, P_2	Pressure in cylinder chambers
M_p, M_L	Piston and load inertia
$F(v_p)$, B_p,	Coulomb friction & viscous friction coeff.
v_p, v_L	Piston and load center of mass velocity
F_{gp}, F_{gL}	Gravity force on piston and load
B_s, K_s	Damping and stiffness of force sensor
θ	Angle with respect to the horizontal
F_p, F_s	Force acting on cylinder and load (measured)
V_{sv}, i_{sv}	Input voltage and current to servovalve
K_{sv}, $K_{sv,o}$	Servovalve gain and its value for $i_{sv} = 0$
x_d, v_d, F_d	Desired position, velocity and force
e_p, e_F	Position and force error
K_P, K_V, K_F	Position, velocity and force error gain

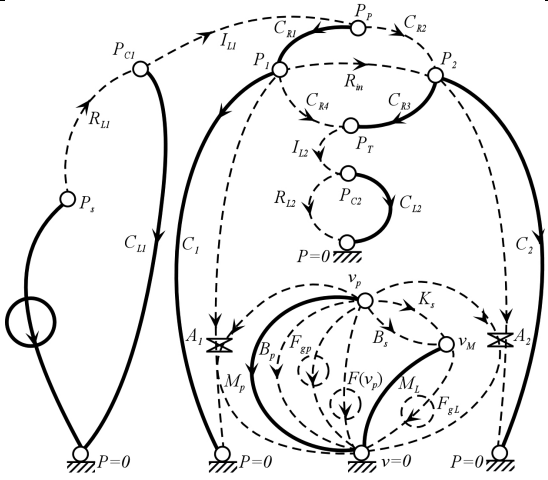

Fig. 3. Electrohydraulic servosystem full model.

The servovalve pressure drop and flow variables P_{R1}, Q_{R2}, P_{R3} and Q_{R4} are associated with the state

variables through pressure drop and flow equations as result of application of the compatibility and continuity laws, respectively and of algebraic manipulations. It has been assumed that the transfer of power is exclusively from the hydraulic system to the load. Other assumptions related to physical limitations are presented in [18].

CONTROL

Having the detailed servosystem model, several position and force control laws were set up and evaluated using MATLAB/ Simulink.

Control System Setup

The custom-designed benchmark setup shown in Fig. 4 was built at the NTUA to test the proposed controller. The particular design of the setup allows for easy changes in the static and dynamic components of the inertial load, driven by the hydraulic actuator. This is achieved by varying the angle of the cylinder with respect to the horizontal and by changing the cylinder-see inertia, by adding or removing weight.

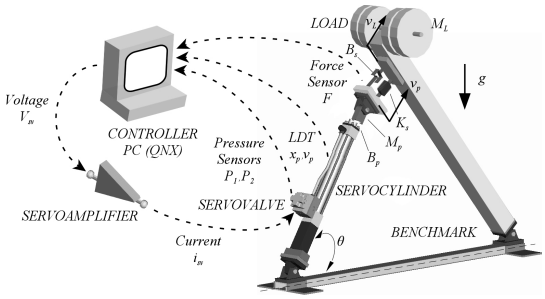

Fig. 4. Schematic of control system setup and benchmark.

A MOOG G122-202A1 Series controller is used to read the servocylinder headside and rearside pressure (from two pressure sensors on the valve manifold), and the piston rod position and velocity (from the built-in analog LDT). A force cell at the end of the rod will provide the load force. The controller card will be interfaced to a PC running the QNX real-time operating system. To use nonlinear and model-based controllers, the PID control section of the card will be by-passed and the card will be used only for reading sensors measurements and for sending the appropriate control voltages to the servoamplifier. The servoamplifier in turn will send appropriate input currents to the servovalve.

Hydraulic Servoactuator Description for Control

In order to provide an equation sufficient for control purposes Eqs. (8) and (9) are combined by taking the difference of pressure derivatives P_1 and P_2 between the cylinder chambers multiplied by the headside and rearside sides, respectively,

$$\dot{F}_p = (Q_{R1} - Q_{R4})A_1/C_1 + (Q_{R3} - Q_{R2})A_2/C_2 + \\ -A_p v_p - R_{in}(A_1/C_1 + A_2/C_2)P_L \quad (15)$$

where by definition, the first part of the resultant equation is the derivative of cylinder output force and $A_p = A_1^{\,2}/C_1 + A_2^{\,2}/C_2$, while the flows to and from the servovalve, from the application of continuity law, have been written as

$$Q_{L1} = Q_{R1} + Q_{R2} \\ Q_{L2} = Q_{R3} + Q_{R4} \quad (16)$$

For deriving the control law, the servovalve orifice conductances are estimated as a linear function of the input current. For positive input commands these are given by

$$G_{R,P\to A}(i_{sv}) = K_m \cdot i_{sv} + C_{R,o}^{-1/2} \\ G_{R,P\to B}(i_{sv}) = -K_l \cdot i_{sv} + C_{R,o}^{-1/2} \quad (17)$$

where $C_{R,o}$ has a very large value, which refers to the resistance of the orifice at servovalve closure, and K_m and K_l are positive constants, which correspond to the main and leakage flow path, respectively. For negative input commands K_m and K_l in Eq. (17) are reversed.

Using Eq. (15), flow/pressure through an orifice equations, Eq. (1), and Eqs. (17), it can be written

$$\dot{F}_p + A_p v_p - K_{sv,o} = K_{sv} \cdot i_{sv} \quad (18)$$

where the cylinder internal hydraulic losses have been neglected due to servocylinder design and the use of special seals and glands that minimize these losses. Thus, the servovalve gain K_{sv} and $K_{sv,o}$ are defined by the equation

$$K_{sv} i + K_{sv,o} = (Q_{R1} - Q_{R4})A_1/C_1 + (Q_{R3} - Q_{R2})A_2/C_2 \quad (19)$$

The terms K_{sv} and $K_{sv,o}$ depend on orifice conductance, the position of the piston rod, which modifies the capacitance of cylinder chambers, the servovalve inlet and outlet pressure and the cylinder chambers pressures. Provided that the pump and tank pressures can approximate the inlet and outlet pressure of the servovalve, respectively, K_{sv} and therefore $K_{sv,o}$ are simplified. However, three variables have to be measured to calculate estimates of K_{sv} and $K_{sv,o}$. Using conductances, Eq. (19) results in

$$K_{sv} i_{sv} + K_{sv,o} = \left(G_{R,P\to A}\sqrt{P_s - P_1} - G_{R,P\to B}\sqrt{P_1}\right)A_1/C_1 + \\ + \left(G_{R,P\to A}\sqrt{P_2} - G_{R,P\to B}\sqrt{P_s - P_2}\right)A_2/C_2 \quad (20)$$

Replacing the G_R according to Eq.(17), (20) yields

$$K_{sv}(P_1,P_2,P_3) = K_m(A_1/C_1\sqrt{P_S - P_1} + A_2/C_2\sqrt{P_2}) \\ + K_l(A_1/C_1\sqrt{P_1} + A_2/C_2\sqrt{P_S - P_2}) \\ K_{SV,o}(P_1,P_2,P_S) = C_{R,o}^{-1/2}[A_1/C_1(\sqrt{P_S - P_1} - \sqrt{P_1}) \\ + A_2/C_2(\sqrt{P_2} - \sqrt{P_S - P_2})] \quad (21)$$

Cylinder force F_p in Eq. (12) is expressed as the sum of the required force to accelerate the piston F_{Mp}, the viscous and Coulomb friction F_{fr}, the gravity force acting on piston and the load applied force F_s measured by a force sensor

$$F_p = F_{Mp} + F_{fr} + F_{gp} + F_s \quad (22)$$

The measured force F_s in Eq. (14) is the sum of the required acceleration force F_{ML} and the gravitational force F_{gL}

$$F_s = F_{ML} + F_{gL} \tag{23}$$

Since the natural frequency of the force sensor is orders of magnitude higher than any other exhibited in the system it is assumed that $v_p \cong v_L$. Substituting Eqs. (22) and (23) in Eq. results in

$$\begin{aligned}\left(M_p + M_L\right)\ddot{v}_p + \left(M_p + M_L\right)g\cos\theta + \\ + B_p\dot{v}_p + A_p v_p - \overline{K}_{sv,o} = \overline{K}_{sv}\cdot i_{sv}\end{aligned} \tag{24}$$

which can be used to describe the electrohydraulic actuator when the resulting motion is of concern.

In most cases, the load mass is orders greater than the piston mass, i.e., $M_L + M_p \cong M_L$. This assumption, together with $v_p \cong v_L$, and Eqs. (23), (24), lead to a useful description of the hydraulic servoactuator dynamics for force control, i.e.

$$\dot{F}_s + B_p\dot{v}_p + A_p v_p - \overline{K}_{sv,o} = \overline{K}_{sv}\cdot i_{sv} \tag{25}$$

where the whole inertia is assigned at the load.

Force Control

The force tracking performance of the proposed model-based force controller is evaluated on the full hydraulic servosystem, described by Eqs. (6)-(14), using MATLAB/Simulink. A constrained task and a free motion task are investigated next.

In the first case, where the motion of the piston rod is considered constrained by a physical obstacle, e.g., a wall, it is assumed that both the velocity and the acceleration of the piston rod are zero. This assumption simplifies Eq. (25) and reveals that the input command modifies only the magnitude of the derivative of the measured force

$$\dot{F}_s - \overline{K}_{sv,o} = \overline{K}_{sv}\cdot i_{sv} \tag{26}$$

By setting the input current command for model-based force control of the constrained cylinder as

$$i_{sv}^{MBFC} = \left(\dot{F}_d + K_F\left(F_d - F_s\right) - \overline{K}_{sv,o}\right)/\overline{K}_{sv} \tag{27}$$

where the desired force F_d is given by

$$F_d = F_{dL} + \overline{F}_{gL} \tag{28}$$

where F_{dL} is the net desired force applied by the cylinder on the load and $\overline{F}_{gL}$ is an estimate of the gravitational force on the load. Defining the force error as $e_F = F_s - F_d$ and provided that the estimates of $\overline{K}_{sv}$, $\overline{K}_{sv,o}$ and $\overline{F}_{gL}$ are accurate, Eq. (27) becomes

$$\dot{e}_F + K_F\cdot e_F = 0 \tag{29}$$

which guarantees exponential force convergence. With $K_F = 100$, and taking into account that the time constant in Eq. (29) is $\tau = 1/K_F$, consistency between expected and simulated responses results (see Fig. 5.a). The overshoot in Fig. 5.a is due to the earlier hypothesis of lumping piston mass to the load. Small transients near the steady state are due to small piston motions. Note that the piston is not still, since the servovalve oscillates around its midpoint in order to let the pressures in cylinder chambers to change, so as to provide the desired load pressure drop, see Fig. 5.b.

In the case of free motion, velocity and acceleration in Eq. (25) cannot be neglected, and have to be compensated. Setting the input current for model-based servoactuator force control in free motion as

$$\begin{aligned}i_{sv}^{MBF} = \left(\overline{B}_p\dot{v}_p + \overline{A}_p v_p + \dot{F}_d + \right. \\ \left. + K_F\left(F_d - F_s\right) - \overline{K}_{sv,o}\right)/\overline{K}_{sv}\end{aligned} \tag{30}$$

where the desired force is defined as in Eq. (28) and provided that the estimation of viscous friction coefficient $\overline{B}_p$ and of the term $\overline{A}_p$ are accurate, Eq. (25) becomes a first order system, as in Eq. (29).

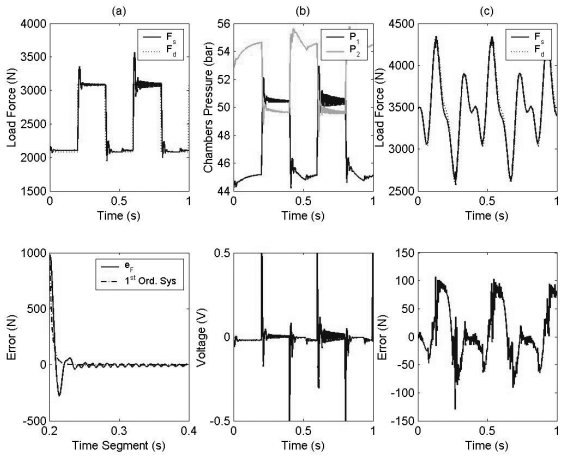

Fig. 5. a) Simulated and desired force and error in time segment 0.2-0.4 s, with model-based control for constrained rod and response of an equivalent 1st order system, b) Simulated cylinder pressure and input voltage command, c) Simulated & desired force and error with model-based control in free motion.

The need of measuring the acceleration of the piston rod can be tackled by calculating the acceleration from Newton's second Law and force sensor measurements as

$$v_p \cong v_L = \left(F_s - F_{gL}\right)/M_L \tag{31}$$

In Fig. 5.c tracking of a desired random force is quite satisfactory and the simulation results show that the proposed model-based controller is promising in providing force control of hydraulic servosystems, given that the physical key systems of the hydraulic servosystem are accurately modeled through intensive experimental procedure. Force error is not zero probably due to the approximations and assumptions made regarding the system dynamics and due to uncertainties in estimating various parameters that have to be compensated and/ or calculated.

Motion Control

Next, the force controller is used to apply the force necessary to accelerate the load along a desired trajectory. Briefly, the desired force, defined in Eq. (28), is now set as

$$F_d = M_L\ddot{x}_d + M_L\left(K_V\cdot\dot{e}_p + K_P\cdot e_p\right) + \overline{F}_{gL} \tag{32}$$

Manipulating the dynamic equation and the input current command for force control, Eqs. (25) and (30), substituting the desired force as given in Eq. (32), and assuming that the measured force tracks the desired force fast and precisely, which can be considered valid as evidenced by the results in Fig. 5.c, then the resulting error system dynamics are approximated by a homogeneous 2nd order system

$$\ddot{e}_p + K_V \cdot \dot{e}_p + K_P \cdot e_p = 0 \qquad (33)$$

which guarantees tracking error convergence to zero, as long as the gains of position and velocity error, K_P and K_V, respectively, are positive. The particular error response is controlled by the selection of K_P and K_V.

The proposed model-based controller was compared to a fixed gain classical PD controller. Gain selection was made so as to ensure a 2nd order system response with critical damping and natural frequency of $\omega_n = 10\,\text{rad/s}$. The performance of the proposed model-based controller is satisfactory regardless of the static and dynamic load variations, see Fig. 6.a. The response of the hydraulic system is similar to the one expected theoretically, i.e. it results in a response of an equivalent 2nd order system for the same position error input. Small oscillations and discrepancies from the expected position error response is due to differences between the real and estimated values in the feedforward terms, see Eq. (30).

Moreover, as shown in Fig. 6.a, a comparison between a classical PD and the proposed model-based controller proves the supremacy of the latter in absolute position error, especially when the inertia of load changes. Nevertheless, not only the tracking accuracy of the desired trajectory is higher with the proposed model-based controller over a classical controller, but also the phase shift is smaller as the frequency of the desired motion is getting higher. In Fig. 6.b, the proposed controller is compared against a classical PD controller for frequencies from 1 Hz to 10 Hz. The superiority of the model-based controller is once again obvious.

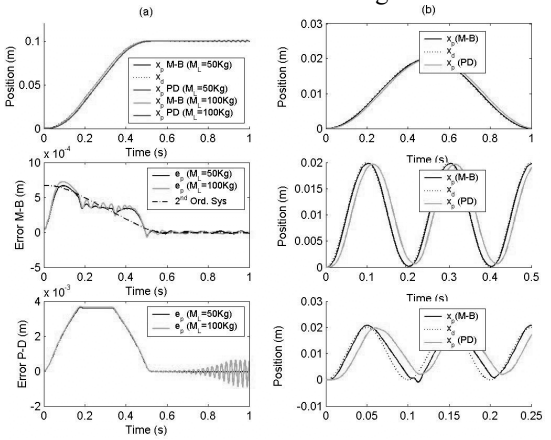

Fig. 6. (a) Simulated and desired piston position and error with model-based control and PD control and position error, (b) Linear PD and proposed model-based controller tracking performance for various frequencies.

CONCLUSIONS

A model-based controller was developed for a high performance electrohydraulic servosystem to improve its position and force tracking performance. The controller was tested on a fully detailed model of the system using MATLAB/ Simulink. Position and force tracking was excellent despite variations of load static and/or dynamic components, making the strategy to be promising in providing robust control to hydraulic manipulators and motion simulators.

REFERENCES

1. Merritt, H. E., *Hydraulic Control Systems*, J. Wiley, 1967.
2. Alleyne, A. et al., "On the Limitations of Force Tracking Control for Hydraulic Active Suspensions", *Proc. American Control Conference*, Philadelphia, Pennsylvania, June 1998.
3. Li, D. and Salcudean, S. E, "Modeling, Simulation and Control of a Hydraulic Stewart Platform", *Proc. IEEE Int. Conf. On Robotics and Automation*, April 1997.
4. Daachi, B. et al., "A Stable Neural Adaptive Force Controller for Hydraulic Actuator", *Proc. IEEE Int. Conf. On Robotics and Automation*, Seoul, Korea, May 2001.
5. Alleyne, A. and Hedrick, J. K., "Nonlinear Adaptive Control of Active Suspension", *IEEE Trans. Control Systems Technology*, Vol. 3, No. 1, 1995.
6. Bu, F. and Yao, B., "Integrated Direct/Indirect Adaptive Robust Motion Control of Single-Rod Hydraulic Actuators with Time-Varying Unknown Inertia", *Proc. IEEE/ASME Int. Conf. Adv. Intelligent Mechatronics*, Como, Italy, 2001.
7. Sirouspour, M. and Salcudean, S. E., "On the Nonlinear Control of Hydraulic Servosystems", *Proc. IEEE Int. Conf. On Robotics & Automation*, San Francisco, CA, April 2000.
8. Six, Klaus, et al., "A Time Delayed Dynamic Inversion Scheme for Mechatronic Control of hydraulic Systems", *Proc. IEEE/ASME Int. Conf. On Advanced Intelligent Mechatronics*, Como, Italy, 2001.
9. Sohl, G. A. and Borrow, J. E., "Experiments and Simulations on the Nonlinear Control of a Hydraulic Servosystem", *IEEE Trans. On Control Systems Technology*, Vol. 7, March 1999.
10. Zhu, W. H., et al., "Emulation of a Space Robot Using a Hydraulic Manipulator on Ground", *Proc. IEEE Int. Conf. On Robotics and Automation*, Washington, DC, May 2002.
11. Honegger, M. and Corke, P. "Model-Based Control of Hydraulically Actuated Manipulators", *Proc. IEEE Int. Conf. On Robotics and Automation*, Seoul, Korea, May 2001.
12. Rowell, Derek and Wormley, David N., *Systems Dynamics: An Introduction*, Prentice Hall, 1997.
13. Watton, John, *Fluid Power Systems*, Prentice Hall, 1989.
14. Blackburn, J. F., et al., *Fluid Power Control*, Technology Press of MIT & John Wiley, 1960.
15. Papadopoulos, E., and Gonthier, Y., "On the Development of a Real-Time Simulator Engine for a Hydraulic Forestry Machine", *Int. J. of Fluid Power*, Vol. 3, No. 1, April 2000.
16. Papadopoulos, E., et al., "Modeling and Identification of an Electrohydraulic Articulated Forestry Machine*", IEEE Int. Conf. on Robotics & Autom.*, Albuquerque, NM, April 1997.
17. MOOG Inc., *Techn. Bull. 117*, Control Div., E. Aurora, NY.
18. Chatzakos Panagiotis, "Design, Modeling and Control of a High-Performance Electrohydraulic Servosystem", *Master Thesis*, in Greek, NTUA, 2002.